Theoretical Study of Optical Transition Matrix Elements in InGaN/GaN SQW Subject to Indium Surface Segregation

Journal:	*Journal of Selected Topics in Quantum Electronics*
Manuscript ID:	JSTQE-CON-SL-04092-2010.R1
Manuscript Type:	Contributed
Date Submitted by the Author:	n/a
Complete List of Authors:	Klymenko, Mykhailo; Kharkov National University of Radio Electronics, Lab. Photonics Shulika, Oleksiy; Kharkov National University of Radio Electronics, Lab. Photonics Sukhoivanov, Igor; University of Guanajuato, DICIS
Keyword:	Nitrogen compounds, Quantum well lasers, Quantum wells, Piezoelectric semiconductors, Piezoelectric devices

Theoretical Study of Optical Transition Matrix Elements in InGaN/GaN SQW Subject to Indium Surface Segregation

Mykhailo V. Klymenko *Graduate Student Member, IEEE*, Oleksiy V. Shulika, *Member, IEEE*
Igor A. Sukhoivanov, *Senior Member, IEEE*

***Abstract*—We investigate the dependence of dipole matrix elements for InGaN/GaN single quantum well structures on the indium surface segregation. Obtained results show that the influence of the surface segregation on the dipole matrix element is not equal for all optical transition. This effect results from the joint action of the piezoelectric polarization and indium surface segregation which change selection rules. In addition, surface segregations at each interface of the quantum well have different impact on optical characteristics depending on the direction of the piezoelectric polarization. The effect of the surface segregation has been estimated applying the global sensitivity analysis in the frame of six-band approximation for the valence band and parabolic approximation for the conduction band.**

***Index Terms*—Indium surface segregation, transition matrix element, piezoelectric polarization, envelope function, global sensitivity analysis**

I. Introduction

THE indium surface segregation (ISS) appears during the crystal growth due to large difference between free binding enthalpies of GaN and InN semiconductor materials [1]. A manifestation of the effect is dependent on the method of crystal growth. However, it is reported [2] that both the molecular beam epitaxy and metalorganic vapour phase epitaxy are accompanied by the ISS.

The ISS can be observed using the transmission electron microscopy (TEM) [3] , reflection high-energy electron diffraction (RHEED) [4] and X-rays diffraction (XRD) [5]. However, all these experimental methods suffer from shortcomings in the case of ultrathin quantum wells (QWs). TEM induce an additional local strain in the crystal lattice after a long duration of the electron beam exposition [6]. Therefore, this experimental technique contains systematic errors. In addition, this method requires special sample preparation. RHEED can be applied only during the crystal growth, and it is not applicable when the growth is over. The XRD technique has low sensitivity for distances up to 2 nm and its experimental data are difficult to interpret. Thus, all these methods have many restrictions in the case of ultrathin InGaN/GaN QWs with thickness smaller than 5 nm. The optical spectroscopy allows to avoid most of these disadvantages. However, the application of this experimental technique requires the mathematical model giving an interpretation of measured spectroscopic data. Such a model of the optical response should provide clear relationship between optical spectroscopic data and parameters of structure imperfections. In this paper, we investigate the influence of the ISS on the dipole matrix elements defining the selection rules for optical intraband transitions. Magnitudes of dipole matrix elements reflect peak intensities of absorption spectra of semiconductor heterostructures.

The structure under consideration is 2 nm InGaN/GaN single QW with strain effects, piezoelectric polarization and ISS. In this paper, the influence of the ISS is studied for each front of the QW separately. For this purpose, we apply the global sensitivity analysis to estimate the sensitivity of dipole matrix elements to variations of ISS parameters. The analyze is applied for optical transitions between all possible pairs of subbands in the QW.

In section II, we will consider two approaches to parametrization and modeling of the indium distribution. Next, in Section III, we will describe the approach to modeling of position-dependent material parameters and piezoelectric polarization in InGaN/GaN QW structure. Section IV contains results of band structure computations. In Section V, we will present the theory of the dipole matrix element, its dependence on the in-plane wave vector and results of the global sensitivity analysis. Section VI contains conclusions.

II. Indium distribution profile

The experimentally observed indium distribution in InGaN/GaN QW structures is determined by the set of phenomena which occur at interfaces of the QW. Approaches to modeling and parameterizing of this indium distribution depends on which phenomenon is prevailed in considered structure under defined physical conditions. For an example, the interdiffusion of indium, resulted from high-temperature annealing, is described by the Fick's law [7]. In this case, the indium distribution profile expressed as a linear combination of the complementary error functions.

It is possible to use the Gaussian function for the approximation of QWs potential profile with the ISS. In this case, the width of the Gaussian function is a fitting parameter, which can be found from experimental data or theory treatment.

This work is partially supported by Dirección de Apoyo a la Investigacón y al Posgrado de la Universidad de Guanajuato under grant # 000041/10

M. V. Klymenko is with Lab. "Photonics", Kharkov National University of Radio Electronics, Kharkov 61166, Ukraine(e-mail: klymenko@daad-alumni.de)

O. V. Shulika is with Lab. "Photonics", Kharkov National University of Radio Electronics, Kharkov 61166, Ukraine(e-mail: a.shulika@osamember.org)

I. A. Sukhoivanov is with DICIS, University of Guanajuato, Com. Palo Blanco, Salamanca, 36885, Gto, Mexico (e-mail: i.sukhoivanov@ieee.org).

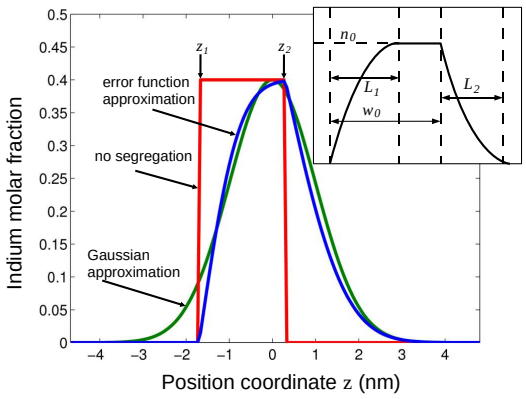

Fig. 1. Calculated indium distribution profiles and their parametrization

The Gaussian approximation gives a symmetric distribution of indium. However, TEM images of QW structures suggest that the ISS leads to the asymmetric profile of the indium distribution. Therefore, we use more accurate description based on the combination of error function [1], which result from the kinetic equations [8]:

$$n_{In}(z) = \begin{cases} 0, & z \le z_1 \\ n_0 \mathbf{erf}\left(\frac{w_0}{L_1}\right)\left[1 - \mathbf{erf}\left(\frac{z-z_2}{L_2}\right)\right] & z \ge z_2 \\ n_0 \mathbf{erf}\left(\frac{z-z_1}{L_1}\right) & \text{otherwise} \end{cases} \quad (1)$$

here: $n_{In}(z)$ is the indium distribution, n_0 is the nominal indium molar fraction in QW layer, L_1 and L_2 are the lengths of the surface segregation, $w_0 = z_2 - z_1$, w_0 is the nominal width of QW.

This formula leads to the indium distribution, that is in good agreement with published experimental results *et al*, [9], [10]. As one can see form Fig. 1 the expression (1) gives asymmetric indium distribution. This approximation contains two fitting parameters L_1 and L_2 instead of single one in case of the Gaussian approximation. This gives more freedom to provide accurate fitting and allows to achieve an asymmetrical distribution. Hereafter, we name parameters L_1 and L_2 segregation lengths. As it follows from experimental data, fitting parameters L_1 and L_2 are not equal that means inequality of the segregation effect for switch-on and switch-off regimes of the MBE indium evaporator.

III. Position-dependent material parameters and internal electric fields

In this paper, we consider the single QW structure with layers made of $In_xGa_{1-x}N$ and GaN semiconductors. All position-dependent material parameters have been computed using linear interpolation formulas except for the band gap energy. For the band gaps of alloys, we have used the second order interpolation formula with the bowing parameter. Therewith, material parameters for relevant binary semiconductors have been taken from [11].

A well-known peculiarity of the wurtzite crystal heterostructures is strong internal electric fields caused by spontaneous polarization and piezoelectric effects. In this paper, we neglect

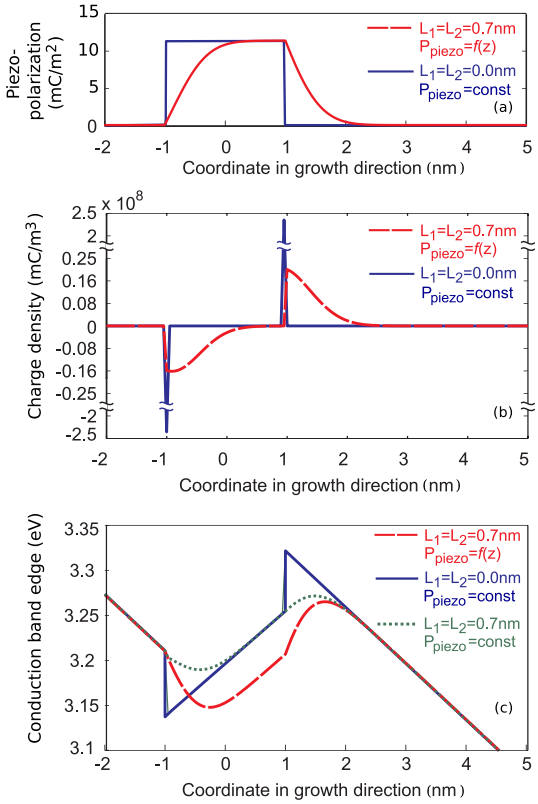

Fig. 2. Positional-dependence of a) piezoelectric polarization, b) piezoelectric charge distribution, and c) conduction band edge for the 2 nm $In_{0.37}Ga_{0.63}N$/GaN quantum well.

the spontaneous polarization and focus our attention on the piezoelectric polarization.

The piezoelectric polarization P_{piezo} is calculated using Vegard's interpolation formula [12]:

$$P_{piezo}(z) = xP^{InN}_{piezo}[\varepsilon(z)] + (1-x)P^{GaN}_{piezo}[\varepsilon(z)] \quad (2)$$

where the strain coefficient $\varepsilon(z)$ is defined as

$$\varepsilon(z) = \frac{a_{subs} - a(z)}{a(z)} \quad (3)$$

here a_{subs} is the lattice constant of the substrate and $a(z)$ is the lattice constant of the unstrained semiconductor alloy at a point z.

The piezoelectric polarization of binary strained semiconductors can be expressed as:

$$P^{InN}_{piezo}[\varepsilon(z)] = -1.373\varepsilon(z) + 7.559\varepsilon^2(z) \quad (4)$$

$$P^{GaN}_{piezo}[\varepsilon(z)] = -0.918\varepsilon(z) + 9.541\varepsilon^2(z) \quad (5)$$

The negative divergence of the polarization gives the volume charge density. Solving the Poisson equation with obtained charge distribution, one can get the potential profile of band edges.

As follows from Eqs. (2)-(5), the ISS leads to the positional-dependence of the piezoelectric polarization. For the structures with zero ISS, the piezoelectric polarization is approximately constant within the QW. Fig. 2 contains results of computations of the piezoelectric polarization, piezoelectric charge

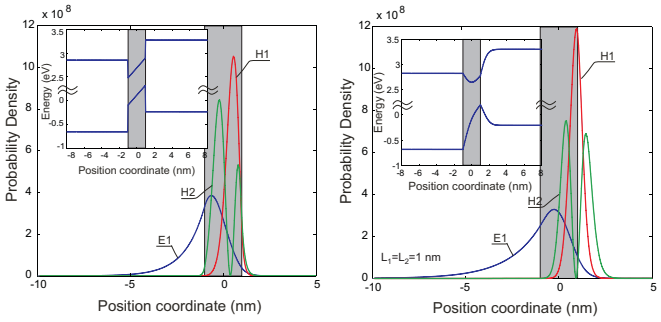

(a) without surface segregation (b) with surface segregation

Fig. 3. Influence of the ISS on envelope function corresponding to the 1st state in the conduction band (E1), 1st (H1) and 2nd (H2) states in the valence band. Shaded areas show nominal thickness of the QW-layer.

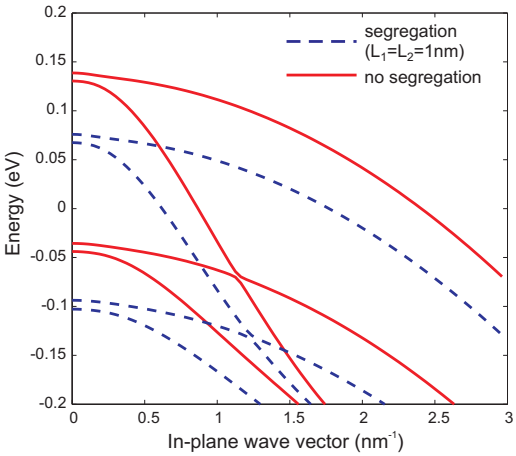

Fig. 4. Band structure of the InGaN/GaN single quantum well without indium surface segregation (solid lines) and with indium surface segregation (dashed lines) for $L_1 = L_2 = 1$ nm.

distribution and conduction band potential profile for several possible approximations. Total neglecting of the ISS leads to the constant piezoelectric polarization and zigzag potential profile of the band edge. Such a shape of the band diagram is caused by the joint action of the piezoelectric polarization in the QW and the electric field of the space charge in doped semiconductor layers. The ISS influences both on the band gap profile and configuration of the piezoelectric field. If only the effect on the band gap is considered and the piezoelectric field is approximated by the constant value, one gets the blue shift of the QW's potential profile relative to its position in the case when the total ISS effect is taken into account. This energy shift is equal 40 meV for the 2 nm $In_{0.37}Ga_{0.63}N$/GaN QW.

The envelope functions corresponding to the center of the Brillouin zone are shown in Fig. 3. Despite of strong modification of the potential profile (Fig. 3(b)), the ISS has not significant influence on envelope functions for first conduction and valence subbands. In this case, a small delocalization is observed, and peaks of both envelope functions are slightly shifted towards the second interface of the QW (Fig. 3(b)). The effect on the second valence subband is more pronounced and valuable. For this subband, the probability density has two maxima which are non-equal in the structure without the ISS. In this case, ratio between maximal values amounts 3:2. The ISS effect equalizes peaks of the probability density having almost equal magnitudes of maxima. We will show further that this feature manifests itself in optical dipole matrix elements.

IV. Band structure

The electron wave function can be obtained solving the Ben-Daniel-Duke equation that is resulted from joint action of the single-band and the envelope function approximation [13], [14]. The valence band structure is computed separately using the six-band model taking into account interactions between heavy holes, light holes and spin-orbit split-off holes states with all possible directions of the spin [15]. This approach leads to 6×6 Hamiltonian:

$$\mathcal{H} = \begin{pmatrix} H^U & 0 \\ 0 & H^L \end{pmatrix} \tag{6}$$

with H^U and H^L of the form:

$$H^U = \begin{pmatrix} F & K & -iH \\ K & G & \Delta - iH \\ iH & \Delta + iH & \lambda \end{pmatrix} \tag{7}$$

$$H^L = \begin{pmatrix} F & K & iH \\ K & G & \Delta + iH \\ -iH & \Delta - iH & \lambda \end{pmatrix} \tag{8}$$

here:

$$F = \Delta_1 + \Delta_2 + \lambda + \theta, \quad G = \Delta_1 - \Delta_2 + \lambda + \theta$$

$$\lambda = \frac{\hbar^2}{2m_0}\left(A_1 k_z^2 + A_2 k_t^2\right) + D_1 \epsilon_{zz} + D_2\left(\epsilon_{xx} + \epsilon_{yy}\right)$$

$$\theta = \frac{\hbar^2}{2m_0}\left(A_3 k_z^2 + A_4 k_t^2\right) + D_3 \epsilon_{zz} + D_4\left(\epsilon_{xx} + \epsilon_{yy}\right)$$

$$\epsilon_{xx} = \epsilon_{yy} = \frac{a_{subs} - a}{a}, \quad \epsilon_{zz} = -\frac{2C_{13}}{C_{33}}\epsilon_{xx}$$

$$\epsilon_{xy} = \epsilon_{yz} = \epsilon_{zx} = 0$$

$$K = \frac{\hbar^2}{2m_0} A_5 k_t^2, \quad H = \frac{\hbar^2}{2m_0} A_6 k_t k_z, \quad \Delta = \sqrt{2}\Delta_3$$

$k_t = |\mathbf{k}_{||}|$, A_1, A_2, A_3, A_4, and A_5 are the valence band structure parameters, D_1, D_2, D_3, and D_4 are the deformation potentials, Δ_1, Δ_2, and Δ_3 are the energy parameters, C_{13}, and C_{33} are the elastic stiffness constants.

This problem is further solved numerically, applying the finite difference method [15].

The band structure is presented in Fig.4, where solid lines give the band structure with no segregation, and dashed lines show dispersion curves of the structure subject to the indium surface segregation with segregation lengths $L_1 = L_2 = 1$ nm. One can see energy shift of all states caused by the segregation effect. The blue shift of the transition energy is in agreement with experimental results of other authors [10]. However, it is hard to use this feature to detect and quantitatively estimate the surface segregation, because the shift of all energy states can be caused by many other physical effects. For example, changes in the width of the QW as well as in the depth affect

the energy spectra in the same manner. So, one should search for another manifestations of the ISS to make it detectable and measurable via optical spectroscopy.

V. Interband optical transition matrix elements

Interband optical transition matrix elements (MEs) are key ingredients in estimation of gain and absorption. Therefore, one can expect that manifestation of ISS in MEs could be detected using absorption spectroscopy. Depending on geometry of absorption measurement only TE or both TE and TM matrix elements will contribute in absorption. Therefore, we analyze here both kinds of polarization.

QW under consideration contains four hole subbands and one electron subband. Matrix elements for optical transitions between those subbands are shown in Fig. 5 calculated for different segregation lengths. MEs for wurtzite QW is calculated as given by Chuang [16].

The ISS influences MEs in unequal degree for different in-plane wave vectors. In case of the TE polarization, the effect of the ISS is more observable for small in-plane wave vectors. In the case of the TM polarization, most effects appear at large in-plane wave vectors. Thus, these results suggest to use probe light perpendicular to QW plane to increase measurement precision.

A. Global sensitivity analysis

Overall conclusion of the previous section is that increasing of segregation lengths leads to decreasing of the matrix element. However, segregation at each interface of a QW is not equal. Therefore, to resolve its influence much more data should be analyzed than those presented in Fig. 5. To do that we use here global sensitivity analysis [17]. This approach allow to estimate the sensitivity of the matrix elements with respect to variations of ISS parameters separately and without large number of computations.

Using the global sensitivity analysis we try to clarify how strong the response of the system on the ISS effect is, what ME the most sensitive to the segregation is, and what segregation parameter having the strongest effect on the dipole matrix element is. Final results are expressed as sensitivity coefficients which are defined as:

$$s_{L_m}^{\mu_{ij}} = \frac{\sigma_{L_m}}{\sigma_{\mu_{ij}}} \frac{\partial \mu_{ij}}{\partial L_m} \tag{9}$$

here σ_{L_m} and $\sigma_{\mu_{ij}}$ are standard deviations for segregation lengths and transition matrix elements respectively.

As we found above, TE matrix elements are more useful from practical viewpoint. Therefore, here, we analyze MEs only for zero in-plane wave vector, i.e. at the center of the Brillouin zone. At the center of the Brillouin zone, shapes of the light and heavy hole envelope functions are almost identical. Therefore, we consider only heavy hole states, because results for light holes will be the same. Thus, we compute the dipole matrix elements μ_{11} and μ_{13} for optical transitions between first subband E1 in the conduction band and two heavy hole subbands H1 and H2 instead of full consideration.

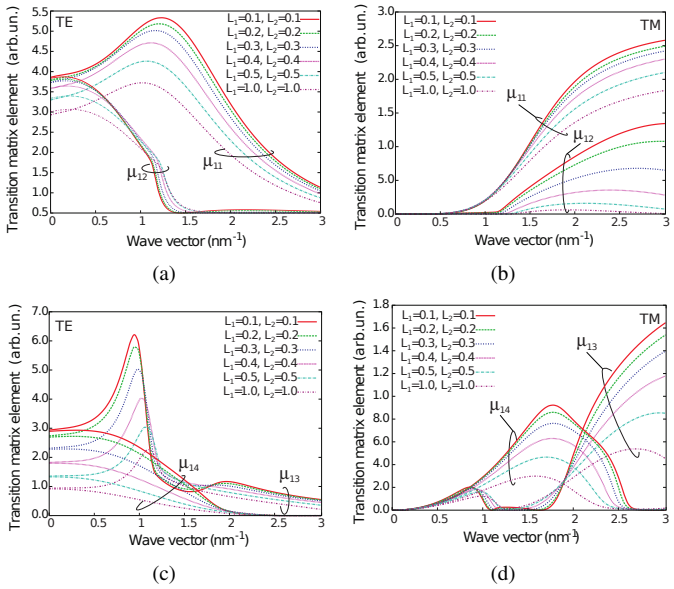

Fig. 5. In-plane wave vector dependence of the dipole matrix elements for (a) TE polarization, transitions E1-HH1 and E1-LH1, (b) TM polarization, transitions E1-HH1 and E1-LH1 and TM, (c) TE polarization, transitions E1-HH2 and E1-LH2 and (d) TM polarization, transitions E1-HH2 and E1-LH2. All curves are obtained for segregation parameters $L_1 = L_2 = 0.1, 0.2, 0.3, 0.4, 0.5, 1.0$ nm.

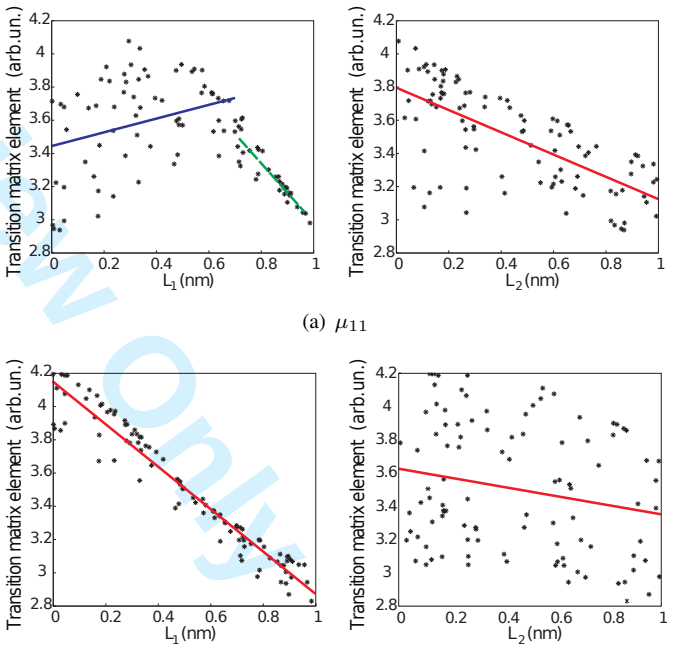

Fig. 6. Global sensitivity analysis of the dipole matrix elements (TE polarization) according to segregation parameters L_1 and L_2

The scatterplot in Fig. 6 (a) reflects the particular feature that the sensitivity of μ_{11} is not the same for all values of L_1. The behavior of the scatterpoints distribution is changed significantly crossing the value $L_1 \approx 0.7$. This means that the sensitivity coefficient is dependent on the segregation length L_1. In this connection, we use approximation based on two linear regressions for ranges $0 \leq L_1 < 0.7$ and $0.7 \leq L_1 \leq 1$

TABLE I
SENSITIVITY COEFFICIENTS

	L_1		L_2
μ_{11}	1.93	for $0 \le L_1 < 0.7$	-1.63
	-3.20	for $0.83 \le L_1 \le 1$	
μ_{13}	-3.38		-0.34

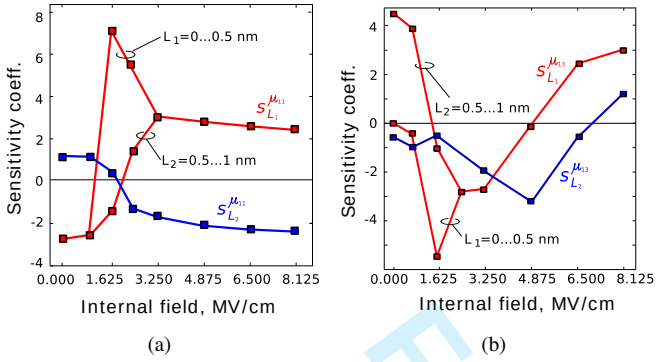

(a) (b)

Fig. 7. Dependencies of the segregation coefficients on intensity of the internal electrostatic fields for dipole matrix elements a) μ_{11} and b) μ_{13} of the 2 nm $In_{0.37}Ga_{0.63}N/GaN$ quantum well

and, consequently, we obtain two sensitivity coefficients.

Table I contains values of sensitivity coefficients. The ISS parameter L_1 has stronger influence comparing with L_2. The dipole matrix element μ_{13} is most sensitive to the indium surface segregation. This behavior can be interpreted looking on envelope functions overlap shown in Fig. (3). The envelope function for second heavy hole states has two extrema which are located near interfaces where the ISS occurs. It makes this subband be especially sensitive to changes of the potential at interfaces of the QW.

Considered above sensitivity coefficients are computed for the 2 nm $In_{0.1}Ga_{0.9}N/GaN$ QW with the piezoelectric field $E_{piezo} = 1.2$ MV/cm and without any other electrostatic fields. In real structures, the QW is surrounded by doped semiconductor layers forming p-i-n structure. Therefore, the QW layer is affected by the electric field of the space charge appeared at interfaces in the doped layers. Sensitivity coefficients for this case are presented in Fig. 7-8. As follows from results in Fig. 7, sensitivity coefficients are strongly dependent on the magnitude of the internal electrostatic field. This field is the superposition of the fields caused by the piezoelectric polarization and space charge on doped layers.

In Fig. 7, sensitivity coefficients $s^{\mu_{11}}_{L_1}$ and $s^{\mu_{13}}_{L_1}$ takes two values in the range from 0.8 to 3.25 MV/cm. In this range, the internal voltage drop across the width of the QW is slightly less than the potential of band offsets. Herewith, the sensitivity coefficients are strongly nonlinear and the scatterplot takes on the appearance of Fig. 6(a). This range of internal fields are most interesting for the optical spectroscopy of the ISS due to high magnitude of the sensitivity to the ISS.

The sensitivity coefficients $s^{\mu_{11}}_{L_1}$ and $s^{\mu_{11}}_{L_2}$ are almost constant at the high internal fields while the sensitivity coefficients $s^{\mu_{13}}_{L_1}$ and $s^{\mu_{13}}_{L_2}$ have non-trivial dependence on the internal field even at high magnitudes. At very low and very high intensities

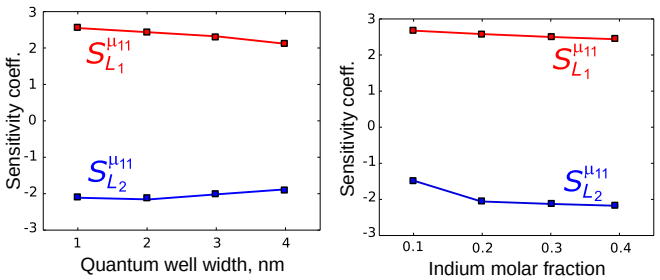

(a) (b)

Fig. 8. Dependencies of the segregation coefficients $s^{\mu_{11}}_{L_1}$ and $s^{\mu_{11}}_{L_2}$ on a) the quantum well width and b) indium amount for the 2 nm $In_xGa_{1-x}N/GaN$ quantum well

of internal fields, the dipole matrix element μ_{11} have opposite sensitivity relative to the ISS at each interface of the QW. This means that the ISS at one interface leads to increasing of the dipole matrix element while the ISS at another interface leads to decreasing of this value. If the segregation lengths L_1 and L_2 are approximately equal, total changes in the dipole matrix element μ_{11} caused by the ISS are very small due to the mutual compensation. It is not the case for the matrix element μ_{13} which is very sensitive to the ISS in these ranges.

Fig. 8 reflects weak dependence of the sensitivity on the QW width and indium amount. Increasing of the QW width leads to the monotonic decreasing of the sensitivity to both segregation lengths. Indium amount determines the depth of the QW and influences on the magnitude of the piezoelectric polarization. As a result, this characteristic is very close to the dependence of the $s^{\mu_{11}}_{L_1}$ and $s^{\mu_{11}}_{L_2}$ on the internal fields.

As far as it is possible to change the magnitude of internal fields managing the doping profile and turning applied electrical bias, considered above sensitivity features could be of interest for the experimental observation of the ISS. All presented results are dependent on the polarity of the QW. Here, we consider only the case of the Ga-face growth.

VI. CONCLUSIONS

In summary, we have investigated the influence of the ISS on the dipole matrix element for InGaN/GaN single QW structures. The joint action of the ISS and internal electrostatic fields leads to pronounced sensitivity of dipole matrix elements to variations of the segregation lengths L_1 and L_2.

The global sensitivity analysis have shown that the transition matrix elements μ_{13} and μ_{14} involving transitions E1-HH2 and E1-LH2 are more sensitive to the ISS comparing with optical transitions E1-HH1 and E1-LH1 subbands.

Dipole matrix elements are most sensitive for the internal fields limited in the ranges from 0.8 to 3.25 MV/cm. For the 2 nm $In_{0.37}Ga_{0.63}N/GaN$ QW, computed intensity of the internal fields is equal $E_{piezo} = 6.2$ MV/cm. In this case, an effective observation of the ISS requires decreasing of this magnitude that can be realized applying of the high-intense reverse voltage bias.

REFERENCES

[1] O. Mayrock, H.-J. Wünsche, and F. Henneberger, "Polarization charge screening and indium surface segregation in (In,Ga)N/GaN single and multiple quantum wells," *Phys. Rev. B*, vol. 62, pp. 16870-16880, 2000

[2] V. Potin, E. Hahn, A. Rosenauer, D. Gerthsen, B. Kuhn, F. Scholz, A. Dussaigne, B. Damilano, and N. Grandjean, "Comparison of the In distribution in InGaN/GaN quantum well structures grown by molecular beam epitaxy and metalorganic vapor phase epitaxy," *J. Crystal Growth*, vol. 262, pp. 145-150, 2004

[3] B. Witzigmann, V. Laino, M. Luisier, U. T. Schwarz, G. Feicht, W. Wegscheider, K. Engl, M. Furitsch, A. Leber, A. Lell, and V. Härle, "Microscopic analysis of optical gain in InGaN/GaN quantum wells," *Appl. Phys. Lett.*, vol. 88, 021104, 3 pages, 2006

[4] S. Martini, A.A. Quivy, T.E. Lamas, M.J. da Silva, and E.C.F. da Silva, "Influence of indium segregation on the RHEED oscillations during the growth of InGaAs layers on a GaAs(0 0 1) surface," *J. Crystal Growth*, vol. 251, pp. 101-105, 2003

[5] S. Pereira, M.R. Correia, E. Pereira, K.P. O'Donnell, E. Alves, A.D. Sequeira, N. Franco, I.M. Watson, and C.J. Deatcher, "Strain and composition distributions in wurtzite InGaN/GaN layers extracted from x-ray reciprocal space mapping," *Appl. Phys. Lett.*, vol. 80, pp. 3913-3915, 2002

[6] T. Li, E. Hahn, D. Gerthsen, A. Rosenauer, A. Strittmatter, L. ReiAYmann, and D. Bimberg, "Indium redistribution in an InGaN quantum well induced by electron-beam irradiation in a transmission electron microscope," *Appl. Phys. Lett.*, vol. 86, pp. 241911, 2005

[7] D. Biswas, S. Kumar, and T. Das, "Band offsets of $In_xGa_{1-x}N$/GaN quantum wells reestimated," *Thin Solid Films*, vol. 515, pp. 4488-4491, 2007

[8] I. Stanlay, G. Coleiny, and R. Venkat, "Theoretical study of In desorption and segregation kinetics in MBE growth of InGaAs and InGaN," *J. Crystal Growth*, vol. 251, pp. 23-28, 2003

[9] K. Muraki, F. Fukatsu, Y. Shiraki, and R. Ito, "Surface segregation of In atoms during molecular beam epitaxy and its influence on the energy levels in InGaAs/GaAs quantum wells," *Appl. Phys. Lett.*, vol. 61, pp. 557-559, 1992

[10] A. Dussainge, B. Damilano, N. Grandjean, and J. Massies, "In surface segregation in InGaN/GaN quantum wells," *Crystal Growth*, vol. 251, pp. 471-475, 2003

[11] I. Vurgaftman, R. Meyer, and L.R. Ram-Mohan, "Band parameters for nitrogen-containing semiconductors",*J. Appl. Phys.*, vol. 94, no. 6, pp. 3675-3696, 2003

[12] V. Fiorentini, F. Bernardini, and O. Ambacher, "Evidence for nonlinear macroscopic polarization in III-V nitride alloy heterostructures," *Appl. Phys. Lett.*, vol. 80, pp. 1204a1206, 2002

[13] G. Bastard, *Wave Mechanics Applied to Semiconductor Heterostructures*. Chichester: John Wiley & Sons Inc., 1991.

[14] W.W. Chow, and S.W. Koch, *Semiconductor Laser: Fundamentals (Physics of the gain materials)*. Berlin: Springer, 1999.

[15] S.L. Chuang, and C.S. Chang, "A band-structure model of strained quantum-well wurtzite semiconductors," *Semicond. Sci. Technol.*, vol. 12, pp. 252-263, 1997

[16] S.L. Chuang, "Optical Gain of strained wurtzite GaN quamtum-well lasers," *IEEE J. Quantum Electron.*, vol. 32, pp. 1791-1800, 1996

[17] A. Salteli et al, *Global sensitivity analysis: a primer*. Chichester: John Wiley & Sons Inc., 2008.

Mykhailo V. Klymenko (GS'09)has received B.S. degree in the area of laser physics and optoelectronic with highest honors from Kharkiv National University of Radio Electronics, Kharkiv, Ukraine, in 2004. After a year he has received M.S. degree. Since 2005, he is PhD student at the Department of Physical Foundations of Electronic Engineering. In 2007 he is awarded by one-year scholarship from German Academic Exchange Service (DAAD)for research in Theoretical Semiconductor Physics Group of Prof. S. W. Koch at Philipps-University, Marburg. His area of interests covers semiconductor optics, quantum field theory, physics of semiconductor nanostructures.

Oleksiy V. Shulika (S'01-M'08) has received both B.S. and M.S. degree in electronic engineering with highest honors from the Kharkiv National University of Radio Electronics, Kharkiv, Ukraine, in 2000 and 2001 respectively, and Ph.D. degree in optics and laser physics from V. N. Karazin National University, Ukraine, in 2008. His research interests are semiconductor optics, physics of semiconductor nanostructures, optoelectronic devices simulation.

He is the Associate Professor at Kharkiv National University of Radio Electronics, Ukraine. From 2005 to 2006 he is visiting researcher at Institute for High-Frequency and Quantum Electronics, University of Karlsruhe (TH), Germany.

Dr. Shulika is Member of IEEE Photonics Society, Optical Society of America, and SPIE, Member of the Organizing Committee of the Conference Series "International Conference on Advanced Optoelectronics and Lasers, CAOL" , NATO Advanced Research Workshop "Terahertz and Mid Infrared Radiation: Basic Research and Applications, TERA-MIR", "International Conference on Laser and Fiber-Optical Networks Modeling, LFNM".

Igor A. Sukhoivanov (M'94-SM'00) has received the M.S. degree in electronic engineering, Ph.D. degree in quantum electronics and fiber optics, both from the Kharkiv Institute of Radio Electronics, and Dr.Sc. in optics and laser physics from V. N. Karazin National University Kharkiv, Ukraine in 1976 , 1985 and 2002 respectively. His research activities concern fiber optics and semiconductor MQW lasers, photonics crystals elements.

Since 1985 he has been an Assistant Professor, Associate Professor and than full Professor of the Faculty of Electronic Engineering, National University of Radio Electronics, Kharkiv, Ukraine. At present he is Professor at the FIMEE, University of Guanajuato, Mexico. From 1987 to 1988, he is a Research Scientist at Humboldt University in Berlin, Germany. In 1994, 1997, and 2002 he is Guest Scientist at the Institute of High Frequency Technique of the Karlsruhe University, Germany, and in 2001 at the Laboratory CEM2, University Montpellier, France. He is the author and co-author of one monograph and over 70 papers in refereed scientific journals.

Prof. Sukhoivanov is Senior Member of IEEE Photonics Society, and Member of the Optical Society of America, APS, SPIE, Organizer and Chairman of the Conference Series "International Conference on Advanced Optoelectronics and Lasers, CAOL", NATO Advanced Research Workshop "Terahertz and Mid Infrared Radiation: Basic Research and Applications, TERA-MIR", etc.

Last name (Family name): Klymenko
First name: Mykhailo
Suffix: Mr.
Affiliation: Lab. “Photonics”, Kharkov National University of Radio Electronics, Lenin avenue 14, Kharkov 61166, Ukriane
Telephone: +38(057)702-13-84
Email: klymenko@alumni-daad.de

Last name (Family name): Shulika
First name: Oleksiy
Suffix: Dr.
Affiliation: Lab. “Photonics”, Kharkov National University of Radio Electronics, Lenin avenue 14, Kharkov 61166, Ukriane
Telephone: +38(057)702-13-84
Email: a.shulika@osamember.org

Last name (Family name): Sukhoivanov
First name: Igor
Suffix: Prof.
Affiliation: DICIS, University of Guanajuato, Com. Palo Blanco, Salamanca, 36885, Gto, Mexico
Email: i.sukhoivanov@ieee.org